A New Technique for Investigating the Biophysical Basis of "Angiogenic Contrast" in Tumors using Susceptibility-based MRI

A. P. Pathak[1], B. D. Ward[2], and K. M. Schmainda[3]

[1]JHU ICMIC Program, Dept. of Radiology, The Johns Hopkins University School of Medicine, Baltimore, MD, United States, [2]Biophysics Dept., Medical College of Wisconsin, Milwaukee, WI, United States, [3]Radiology and Biophysics Depts., Medical College of Wisconsin, Milwaukee, WI, United States

Recently, we and others showed that microvessel geometry is a significant determinant of susceptibility-based contrast. This is especially relevant when imaging tumors with their characteristically anomalous vascular trees. In such cases, the traditional cylindrical perturber (CP) approximations employed by most susceptibility models may be inadequate. Here we describe a novel simulation technique, the *finite perturber model* (FPM) that circumvents shortcomings of traditional fixed-geometry approaches, and enables us to study susceptibility-induced contrast arising from *arbitrary* microvascular geometries in 3D, such as those typically observed during tumor angiogenesis. The excellent agreement of the FPM with theory coupled with its computational efficiency demonstrates its potential to radically transform our understanding of the factors that engender susceptibility contrast in tumors.

INTRODUCTION Several models have been developed to help understand the factors that contribute to susceptibility-induced MR signal change, and quantify its association with the underlying microvascular geometry [2, 3]. However, we recently demonstrated that the grossly different vascular morphology of tumors due to tumor angiogenesis, compared to normal brain, can profoundly influence susceptibility-induced MR contrast [4]. While computationally convenient, the CP approximations employed by most susceptibility models for representing tumor vessels may be inadequate. Traditional CP models also assume the magnetic field is constant along the length of the vessels, allowing such effects to be simulated in 2D. However, any vessel geometry deviating from the cylindrical model would need to be simulated in 3D, since induced field gradients are a function of the 3D microvessel geometry. In addition, the CP approach assumes large inter-vessel separations, so that effects of overlapping field gradients can be disregarded. This assumption may be inappropriate for tumors – wherein vessel density may be low, but due to larger caliber tumor vessels, the inter-vessel distances may not be negligible. Finally, overlapping field gradients may become significant at high contrast agent doses and dominate the eventual image contrast observed. Our original FPM approach [1] circumvented many of the above drawbacks [1], but was computationally less efficient as it employed an "oct-tree" or "nested-cube" data structure for representing the vascular tree. The primary motivations for developing this new FPM approach were to develop a 3D technique applicable to *arbitrarily-shaped* (tumor) microvessels that was computationally more efficient and to gain insight into the biophysics of "angiogenic contrast".

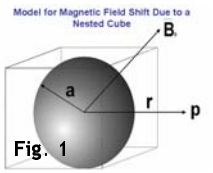

Fig. 1

METHODS ***"Finite Perturber Model (FPM)"*** **For Computing Field Perturbations:** FPM differs from standard numerical methods such as finite differences in that it does not solve Maxwell's equations directly. Instead, the underlying vessel geometry or "substrate" is divided into minute "perturbers". To calculate the field shift at a given point, the shift due to each perturber is calculated independently. The total field shift is then calculated as the sum of the field shifts from all the perturbers. Since we cannot completely fill the vascular geometry using spheres of finite radius due to gaps remaining between spheres, we defined an infinitesimally small cube as the perturber. In order to calculate the magnetic field shift due to a cube of side '*s*', we considered a sphere of radius '*a*', half the length of the side of the cube, embedded in the cube (**Fig. 1**). We then approximated the magnetic field shift for the cube at a test point *p* by:

$$\Delta B_{cube}(p) = \left(\frac{6}{\pi}\right)\frac{\Delta\chi}{3}\frac{a^3}{r^3}(3\cos^2\theta - 1)B_0$$

Where, a = sphere radius, r = dist. from cube center, θ = angle with B_0. As there is a $1/r^3$ dependence of $\Delta B_{cube}(p)$, the error introduced by a coarse approximation to the substrate at a relatively large distance from p is negligible. The above equation yields the magnetic field perturbation from a single finite perturber. To calculate the total field perturbation from the vasculature, we let the radius a of the finite perturber become infinitesimally small, and integrate over the entire space:

$$\Delta B(x,y,z) = \iiint V(\xi,\eta,\zeta)\,\Delta B_{cube}(x-\xi, y-\eta, z-\zeta)\,d\xi\,d\eta\,d\zeta$$

Where, V(x,y,z) is a function that indicates whether the given point is inside the vasculature; i.e.:

$$V(x,y,z) = \begin{cases} 1, \text{if } (x,y,z) \text{ is inside the vasculature,} \\ 0, \text{if } (x,y,z) \text{ is outside the vasculature.} \end{cases}$$

Next, take the 3D Fourier transform of both sides of this equation.

$$\Im\{\Delta B(x,y,z)\} = \Im\left\{\iiint V(\xi,\eta,\zeta)\,\Delta B_{cube}(x-\xi, y-\eta, z-\zeta)\,d\xi\,d\eta\,d\zeta\right\}$$

The above integral is the 3D convolution of the vascular structure with the finite perturber field and can be rewritten as:

$$\Im\{\Delta B(x,y,z)\} = \Im\{V(x,y,z) \otimes \Delta B_{cube}(x,y,z)\}$$

The above is equivalent to:

$$\Im\{\Delta B(x,y,z)\} = \Im\{V(x,y,z)\}\,\Im\{\Delta B_{cube}(x,y,z)\}$$

Taking the inverse Fourier transform of the above equation, we get:

$$\Delta B(x,y,z) = \Im^{-1}\{\Im\{V(x,y,z)\}\,\Im\{\Delta B_{cube}(x,y,z)\}\}$$

This equation is an efficient means of calculating the magnetic field perturbation.

Simulation Procedure: *1*. Convert input representation of vascular structure into a 3D grid. *2*. Calculate 3D magnetic field map corresponding to the finite perturber. *3*. Calculate 3D FFT of the vascular structure. *4*. Calculate 3D FFT of the finite perturber field map. *5*. Perform the point-wise multiplication of two 3D FFT's. *6*. Calculate the inverse FFT of this product. Once computed the field, we modeled proton diffusion by Monte Carlo methods employing a diffusion coefficient (D) of 1.0 μm^2/ms. 10000 protons were randomly placed in the simulation universe with diffusion permitted across vessel walls. The final MR signal was estimated using:

$$S(t) = \frac{1}{N}\sum_{n=1}^{N} e^{j\phi_n(t)}$$

Where, N = no. of protons, $\phi_n(t)$ = phase of nth proton at time t given by:

$$\phi_n(t) = \sum_{j=1}^{t/\Delta t} \gamma \Delta B(p_n(j\Delta t))\Delta t$$

Where, Δt=simulation time step, γ=267.6×10^{6}rad/T, $p_n(t)$=position of nth proton at time t, $\Delta B(p)$ = magnetic field shift at position p. Prior to applying the FPM to the anatomical substrate, we validated its numerical accuracy by comparing it with analytically obtained values of the magnetic field perturbations produced by a cylindrical perturber. The anatomical substrate for our simulations was a digitized 3D representation of a cerebrocortical capillary network (≈70μm^3, kindly provided by Dr. Tony Hudetz, Dept. of Anesthesiology, Medical College of Wisconsin) [5].

RESULTS **Fig. 2** shows numerical result from FPM plotted vs. results from the analytical equation. It can be seen that except for the boundary of the cylinder, there is excellent agreement between the two. **Fig. 3** Inset illustrates the reconstructed cerebrocortical substrate; foreground is the estimated MR signal for susceptibilities typical of deoxygenated blood. Finally, **Fig. 4a** illustrates a slice though the 3D magnetic field map computed for the cerebrocortical substrate – one can clearly see field perturbations around vessels that are qualitatively consistent with classic dipolar patterns, while **Fig. 4b** shows the field isolines for the same slice.

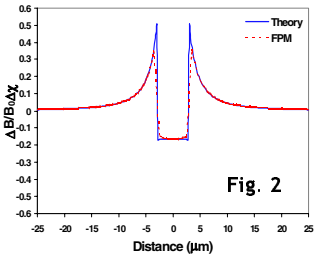

Fig. 2

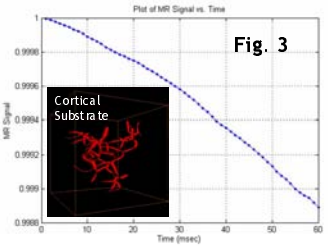

Fig. 3

DISCUSSION/CONCLUSIONS
We have successfully demonstrated both the numerical accuracy and feasibility of a novel technique for estimating the susceptibility-induced MR signal for *arbitrary* microvascular geometries. Further, our technique allows us to visualize these effects in 3D, in exquisite detail, a feat to the best of our knowledge that has not been demonstrated to date. Since this is a work in progress, we are in the process of assessing the effects of tumor angiogenesis on the MR signal and investigating the BOLD contrast mechanism.

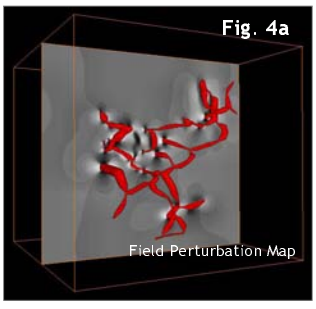

Fig. 4a

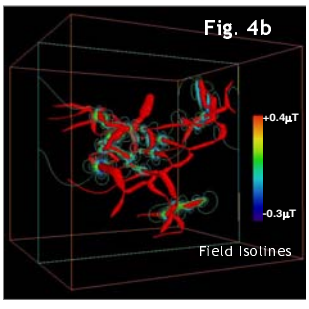

Fig. 4b

References 1. Pathak et al., 1331;ISMRM:2002; **2.** Boxerman et al., *MRM*, 34(4):1995; **3.** Kiselev *MRM*; 46(6):2001; **4.** Pathak et al., *JMRI*; 18(4):2003; **5.** Hudetz et al., *Microvas Res*, 46:293, 1992.